Scientia Iranica A (2014) 21(3), 548–556

Sharif University of Technology
Scientia Iranica
Transactions A: Civil Engineering
www.scientiairanica.com

Dispersion around a circular cylinder in surface wave motion

M.A. Tofighi and M. Jamali*

Department of Civil Engineering, Sharif University of Technology, Tehran, P.O. Box: 11155-9313, Iran.

Received 21 April 2013; received in revised form 4 September 2013; accepted 6 October 2013

KEYWORDS
Water waves;
Flow visualization;
Particle image velocimetry;
Lagrangian dispersion.

Abstract. In this paper, we examine fluid flow and associated dispersion around a circular cylinder under progressive surface wave motion. The flow field and vortex shedding patterns were studied using flow visualization and Particle Image Velocimetry (PIV). Several patterns of vortex shedding were identified around a single cylinder. The vortex shedding patterns under progressive wave motion are similar to those observed in planar oscillatory flow, except in the way the vortices form and in the orientation they take. The observed vortex patterns in progressive wave motion are more unstable than those in planar oscillatory flow. Using particle tracking and the Lagrangian dispersion method, the dispersion coefficients were calculated for various flow regimes. The observations confirm the calculations in general. It was also found that wave steepness can affect the shedding pattern. The vortices tend to shed more frequently in a wave direction at low wave steepness.

1. Introduction

The study of flow patterns around circular cylinders in oscillatory flow has wide applications in engineering, from the design of cylindrical structures against wave forces, in which variation of in-line and lift forces are directly dependent on the vortex shedding pattern, to transport and dispersion in oscillatory environmental flow [1]. An important example of such environmental flow is flow around stems of plants in aquatic canopies by surface wave motion [2]. Surface waves can greatly enhance the dispersion and mixing of nutrients, chemicals, and suspended particles in canopies, and has a direct impact on the circulation of food and other materials in the ecosystem. Many emergent aquatic plants in coastal areas and lakes where surface waves are frequently observed have a round stem free of leaves, so they can be modeled as long cylinders against the flow. To study how dispersion is affected by the presence of aquatic plants, an understanding of dispersion around a single cylinder is essential. Although the hydrodynamics of oscillatory flow around a single cylinder have been studied in detail, e.g. [3], there is a lack of information about how the presence of the cylinder affects the dispersion in such flow. On the other hand, the flow field of a surface wave varies in both time and space, whereas, previous studies focused only on time-dependent flow. These mark the motivation for the present study. Here, we study the flow and the associated dispersion around a single cylinder under surface wave motion, and examine the differences with flow patterns from a purely time-dependent flow.

The structure of the flow around a cylinder in oscillatory flow depends mainly on the Keulegan-Carpenter number (KC $= U_{\max}T/d$) and the Stokes number, or viscous parameter, $\beta = d^2/Tv$, or, alternatively, Reynolds number (Re $=$ KC $\times \beta$), where $U_{\max}$ is the maximum oscillatory velocity, T is the period of

*. *Corresponding author. Tel.: +98 21 66164215; Fax: +98 21 66014828*
E-mail addresses: m.tofighi@gmail.com (M.A. Tofighi); jamali@sharif.edu (M. Jamali)

Table 1. Flow patterns around single circular cylinder in oscillatory time-dependent flows [3,5] and progressive wave (current study).

Williamson [3] (1985)		Obasaju et al. [5] (1988)		Progressive wave (current study)	
KC range	**Pattern**	**KC range**	**Pattern**	**KC range**	**Pattern**
$2 < \mathrm{KC} < 4$	Symmetric non-shedding	–	–	–	–
$4 < \mathrm{KC} < 7$	Asymmetric non-shedding	$4 < \mathrm{KC} < 8$	Asymmetric	$6 < \mathrm{KC} < 8$	Double-shooting
$7 < \mathrm{KC} < 15$	Single-pair[a]	$8 < \mathrm{KC} < 15$	Transverse (single-pair)	$8 < \mathrm{KC} < 15$	Single-pair
$15 < \mathrm{KC} < 24$	Double-pair	$15 < \mathrm{KC} < 22$	Diagonal (double-pair)	$15 < \mathrm{KC} < 24$	Double-pair
$24 < \mathrm{KC} < 32$	Three-pair	$22 < \mathrm{KC} < 30$	Third vortex (three-pair)	–	–
$32 < \mathrm{KC} < 40$	Four-pair	$\mathrm{KC} > 30$	Quasi-steady (four-pair)	–	–

[a]: Single-pair regime means two vortices shed in each period of flow. Other regimes are defined the same way.

oscillation, d is the diameter of the cylinder, and v is the kinematic viscosity of fluid [1]. It is expected that flow regimes around a cylinder remain roughly similar over the range of subcritical Reynolds number ($\mathrm{Re} < 3 \times 10^5$) [3]. Planar oscillatory flow around an isolated circular cylinder was visualized by [3-6]. In experiments conducted by Williamson [3] (1985), a circular cylinder was oscillated in still water and six predominant flow regimes were identified for $2 < \mathrm{KC} < 40, \beta = 255$ (see Table 1). Obasaju et al. [5] (1988) made observations of flow patterns around a circular cylinder for $4 < \mathrm{KC} < 55$ and $100 < \beta < 1665$. The observations in the two studies were almost the same for a similar range of parameters (Table 1). Numerical simulations of the oscillatory flow around a cylinder were made by [1,7-11]. The numerical simulations, in general, reproduced more details of flow than experimental observations.

The mixing mechanism in wave motion consists of dispersion and turbulent diffusion. Turbulence is mainly the result of flow separation over the cylinder. Dispersion takes place in longitudinal and transverse directions and is the result of combined effects of flow diversion and vortex shedding. Dispersion in pure surface wave motion in the absence of any obstacle was studied by [12-14]. Yasuda [12] (1984) analyzed the longitudinal dispersion process from the start to the stationary stages in an oscillatory current. The time variations of the dispersion coefficient for an instantaneous point and line-source releases were found to be oscillatory [12-13]. Similarly, Law [14] (2000) used random walk simulations and investigated longitudinal dispersion due to the mass drift caused by progressive surface waves in the absence of cylinder(s). He showed that the magnitude of the dispersion coefficient is generally an order of magnitude larger than that due to the Stokes drift alone. A nearly constant dispersion coefficient was obtained, only after a lengthy period of time, to the order of 1000 periods.

This study investigates flow and dispersion around a single circular cylinder in surface wave motion. The focus of previous studies was on the hydrodynamics of time-dependent, oscillatory current around a cylinder. To the best of our knowledge, there are no documented studies visualizing the flow around a circular cylinder in surface wave motion, where the flow varies both longitudinally and temporally, and the associated dispersion. In this work, we present the results of an experimental study of such a flow in a wave tank. We use the Particle Image Velocimetry (PIV) technique to find the velocity field around a cylinder and employ a Lagrangian particle tracking technique to quantify the associated dispersion. Section 2 introduces the laboratory experiments and the Lagrangian method for particle tracking. Results of PIV measurements and flow visualizations are given and discussed in Section 3. Concluding remarks are given in Section 4.

2. Methods

2.1. Laboratory experiments

The flow visualization and PIV measurements were conducted in a 9 m long, 0.3 m wide glass walled wave flume, with a depth of 0.6 m, as shown in Figure 1. A 25 cm long Polyamide cylinder was secured

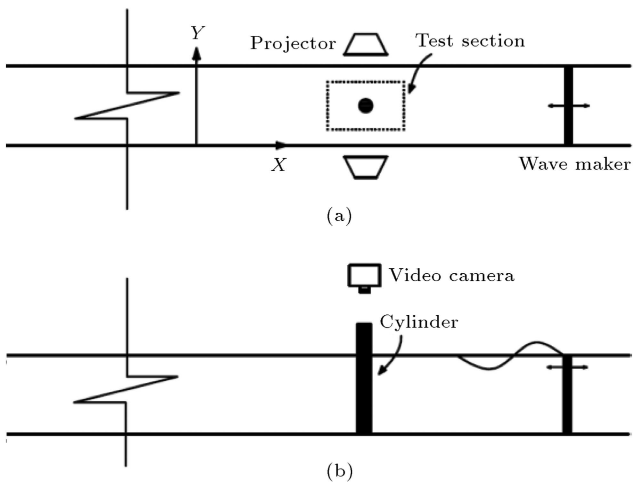

Figure 1. Experimental setup: (a) Top view; and (b) side view.

to a thin false bottom secured in the middle of the channel. Cylinder diameters of $d = 0.63, 1.0, 1.2, 1.5$ and 2.0 cm were tested in the experiments. The water depth, h, was 21 cm, the tested wave periods were $T = 1.14, 1.46$ and 1.86 sec, and the tested wave heights were $H = 3.6, 3.3$ and 1.4 cm; these ranges correspond to $6 < \mathrm{KC} < 24$ and $20 < \beta < 310$. The wave steepness, H/L, where L is wavelength, was less than 2.5% in all the experiments. The cylinder was placed in the center of the test section (see Figure 1(a)).

For PIV, we used a two-mega pixel HD CMOS video camera (SONY-HDR-SR10) installed about 1 m above the water surface and two projectors of 500 W placed at the two sides of the flume. We used $8 - \mu$ m sprinkled glitter powder as the visualization agent on the water surface. We added a small amount of clay to the water to make a body of white colored water. As the clay concentration was below 0.5%, the suspension had negligible effects on water density and kinematic viscosity. When seen from above, the particles looked dark in the background white water (Figure 2). The flow in a test section of about 330×185 mm^2 was recorded in each experiment for at least 20 wave periods, at a rate of 25 frames per second. The video was converted into single images of 1920×1080 pixels^2 using MATLAB. Cross correlation analysis was performed for interrogation areas of 64×64 pixels with 50% overlap to obtain the velocity field. In the case of planar oscillatory flow around a circular cylinder, the normalized lift force frequency (lift frequency/wave frequency) for KC = 24 is 4 [15]. For a wave period of 1.14 sec, the lift frequency (or corresponding vortex shedding frequency) is about 3.5 Hz. The video recording at 25 frames per second (25 Hz) is, therefore, adequate to capture vortex shedding.

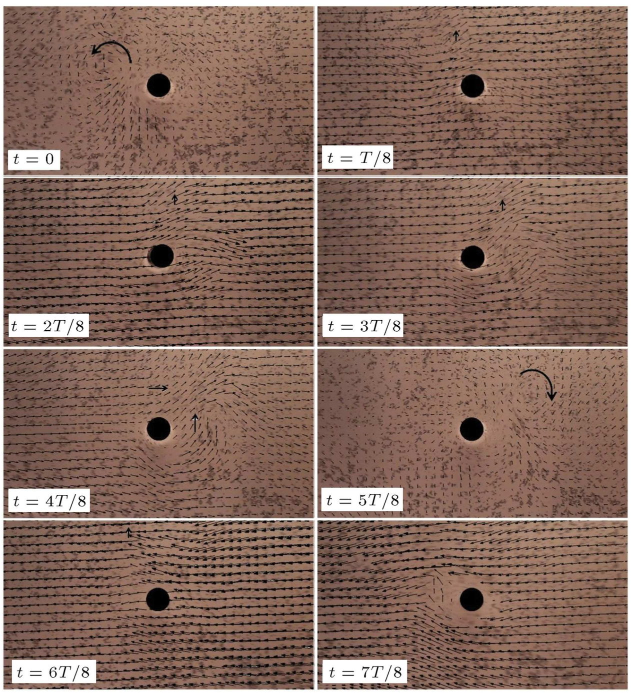

Figure 2. Flow sequence around an isolated cylinder for a full cycle for KC = 9.4 and $d = 1.5$ cm

2.2. The Lagrangian particle tracking method for dispersion calculations

We incorporated the measured velocity fields from PIV into a particle tracking method to calculate the dispersion coefficient in the presence of a cylinder. Dispersion of materials in water flow is mainly the result of molecular diffusion, turbulent diffusion, and shear induced dispersion [16]. When obstacles are present, mechanical diffusion is an additional mechanism [17]. Mechanical diffusion arises from tortuous flow paths of fluid particles between cylinders. This mechanism is common in porous media and aquatic canopy flows, and unsteadiness adds to its complexity, as is the case in this study. In mechanical dispersion, the obstruction of the flow path by soil or plant stems creates variations in flow paths, and the wake regions in lee sides of the obstacles contribute to the dispersion. On the other hand, molecular diffusion and vortex shedding affect the dispersion through particle trapping, and reduce spatial heterogeneity in the local velocity field. The macro-scale dispersion is the result of the combined effects of the above mechanisms. In the particle tracking method, we take a stochastic approach to find a description of the dispersive process, based on the random nature of the smaller-scale data [18]. In a Lagrangian description, the motions of individual fluid elements produce, in sum, the flow field [19].

For the purpose of analysis, we assume each fluid particle moves along a trajectory vector $X = X(t, x_0, t_0)$, where $X = x_0$ when $t = t_0$. The displacement vector of the particle during a time interval of τ is:

$$Y(\tau, x_0, t_0) = X(t_0 + \tau, x_0, t_0) - x_0 = \int_{t_0}^{t_0+\tau} V(t, x_0, t_0)dt, \tag{1}$$

where $V(t, x_0, t_0)$ is the particle velocity at time t given that it was originally at x_0 at time t_0. $Y(\tau, x_0, t_0)$ is a random function of time and an indirect function of space, x_0 [20]. $Y(\tau, x_0, t_0)$ can be decomposed as:

$$Y(t, x_0, t_0) = \langle Y(t, x_0, t_0)\rangle + Y'(t, x_0, t_0), \tag{2}$$

where $\langle Y(t, x_0, t_0)\rangle$ is the expected value (as a function of time) of the displacement, while $Y'(t, x_0, t_0)$ is the displacement fluctuation from the mean value. The angle brackets, $\langle\rangle$, denote the ensemble mean, or average, over many trials.

The second moment tensor $\langle Y_i'(t, x_0, t_0) Y_j'(t, x_0, t_0)\rangle$ is the fluid particle displacement covariance (or variance) [19]. This tensor describes the spread of the particle displacements around the mean motion over time. Differentiating the covariance with respect to time gives the dispersion tensor:

$$D_{ij} = d\langle Y_i'(t, x_0, t_0) Y_j'(t, x_0, t_0)\rangle / dt, \tag{3}$$

which is the average rate of particle spreading over time [18,20-22]. Although $0.5D_{ij}$ is known as the dispersion coefficient tensor [20], we use D_{ij} as a dispersion tendency, or, simply, dispersion tensor, in the rest of this paper.

Particle tracking is a suitable tool for dispersion calculations when the velocity field is completely available. Knowing the trajectories of fluid particles, one can find the tendency of a patch of a conservative tracer to disperse from its initial position. The ensemble mean may be computed by following the released trials in the full domain and averaging the displacement vector over the trials to find the dispersion tensor in the capsulated domain [18,20]. This can also be done by tracking particles released continuously with a small time lag from a fixed point and averaging the displacement vector over time [22]. It is expected that both methods give similar results if the domain is homogeneous. Another interpretation of a particle trajectory vector, as a random variable in time, is the position that one particle takes at some later time. With this definition, the average can be also taken over a period of time in one experiment [16].

The PIV measurement provided the velocity field at a rate of 25 Hz in our experiments. The data can be used to draw the fluid streak lines in the flow field. For accuracy of velocity and better data resolution around the cylinder, we had to limit the video recording window to a certain size. Due to dimensional constraints, a particle released from an arbitrary point may run away from the recording domain over time. Moreover, the released particles near the test section boundaries may escape the test section at an early stage of recording. To overcome these difficulties, we take the trajectory of particles released from a fixed point as a random variable in time [22]. The procedure of calculating the dispersion tensor, thus, becomes as follows:

1. PIV measurements provide the Eulerian velocity fields in the full domain over 20 wave periods at time steps of 0.04 sec (1/25 sec).
2. Virtual particles are released from the same point, each at a time with a time lag of 0.04 sec.
3. The trajectory vector of each particle is calculated from Eq. (1).
4. Care is taken when the particle is close to the cylinder. In these cases, a reflective boundary condition is used to find the trajectory after the particle hits the cylinder.
5. The trajectories are shifted in time, as if the particles were released from the same point at the same time.
6. Displacement vector, covariance, and dispersion tensor are now calculated using Eqs. (2) and (3).

3. Results and discussion

3.1. Flow patterns

Figure 2 shows the flow sequence around an isolated cylinder for a full cycle for KC = 9.4. At $t = 0$ and $t = 5T/8$, a counter-clockwise and a clockwise vortex form in the upper left and the upper right corners of the cylinder at the start of each half cycle, respectively. These vortices are the result of a combination of the transverse flow (see Figure 2, $t = 4T/8$) and the base oscillatory flow. At other times, the velocity field is stronger and the flow has an upward tendency as seen at $t = 3T/8$.

Williamson [3] (1985) investigated the flow structure around a single cylinder in sinusoidally time-dependent flow by monitoring the motion of aluminum powder particles on the free surface. A circular cylinder was oscillated in still water in a tank, and six predominant flow regimes were identified in the range of $2 < \mathrm{KC} < 40$, $\beta = 255$ in his experiments; these are given in Table 1. Obasaju et al. [5] (1988) observed the patterns for the range of $4 < \mathrm{KC} < 55$, $100 < \beta < 1665$. Except for the slight differences in bounds of KC for the given vortex observation, the observations were almost the same for a similar range of parameters in the two studies. Williamson [3] (1985) and Obasaju et al. [5] (1988) state that even when KC and β are fixed, more than one mode of shedding is possible, and the flow may switch between different modes.

In this study, we examine flow patterns around a cylinder in progressive wave motion for the range of $6 < \mathrm{KC} < 24$ and $20 < \beta < 310$. Although small vortices could not be captured, due to apparatus constraints, but the shedding pattern and the stronger vortices were well visualized.

Three predominant vortex shedding patterns were observed around the circular cylinder (Table 1). A schematic of the observed vortices for different ranges of KC are given in Figure 3, with an example of measured vorticity field for each range given in Figure 4. Table 2 summarizes the predominant direction of vortex shedding in these ranges. When $6 < \mathrm{KC} < 8$, two small attached symmetric or asymmetric vortices form in the lee side of the cylinder (see Figure 3(a)). They reach maximum size at the end of the half cycle. When the flow reverses direction, the attached vortices split up and shoot out to the opposite side of the cylinder. These vortices move a maximum distance of $2d$ (see Figure 4(a)) and then lose their strength and

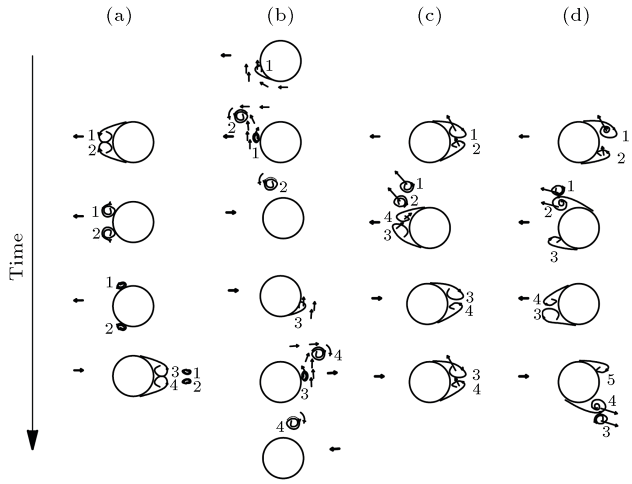

Figure 3. Vortex shedding patterns in progressive wave motion: (a) Double-shooting regime in 6 < KC < 8; (b) single-pair regime in 8 < KC < 11; (c) single-pair regime in 11 < KC < 15; and (d) double-pair regime in 15 < KC < 24. Horizontal arrows show the wave orbital velocity direction.

Table 2. Typical direction of predominant vortex shedding in different flow patterns relative to the wave direction ($\longleftrightarrow$).

KC	Direction	Strength
6 < KC < 8	$\longleftrightarrow$	Weak
8 < KC < 11	$\uparrow$	Strong (vortex street)
11 < KC < 15	$\nearrow$	Strong (vortex street)
15 < KC < 24	$\longleftrightarrow$	Strong

disappear. This pattern repeats in the next half cycle. This mode is named 'double-shooting' for the way the vortices are detached from the cylinder. However, it is essentially similar to the asymmetric and symmetric regimes in time-dependent oscillatory flow (Table 1). In some instances, the vortex of each cycle pairs with the new vortex in the following half cycle to form a single vortex. This is similar to the case KC < 8 in time-dependent oscillatory flow [3].

The single vortex pairs observed in the range 8 < KC < 15 are shown in Figure 3(b) and (c). When 8 < KC < 11, a strong small vortex (vortex (1)) initially forms in the lee side of cylinder (Figure 3(b)). Flow associated with this vortex is nearly perpendicular to the oscillation direction (see Figure 2 at $t = 4T/8$). Vortex (2) is the result of this transverse and the base oscillatory flow. This vortex moves transversely and leaves the cylinder flow field. When flow reverses, vortex (1) disappears and a new attached vortex (3) forms in the other side of the cylinder (Figure 3(b)). Vortex (3) causes a flow sequence similar to vortex (1), but on the other side of the cylinder. Accordingly, vortex (4) is created and leaves the cylinder field transversely in the same direction as vortex (2). Hence, a vortex street forms (Figure 4(b)), as indicated by [3]. When 11 < KC < 15, one pair of vortices forms and leaves the wake field at an angle to the main flow direction (Figure 3(c)). The street direction has a maximum angle of 45° to the wave direction in this case. This regime is basically the single-regime, as described by [3,5]. However, here we found another shedding pattern (compare Figure 3(b) and (c)). It is a formed vortex far from the cylinder due to a strong attached vortex in each cycle (Figure 2 at $t = 0$ and $t = 5T/8$).

In the range of 15 < KC < 24, a pair of vortices shed in each half-cycle. Two trails of vortex pairs convect away from the cylinder from opposite sides of the cylinder and in an opposite direction. Figure 3(d) shows the details of pairing in a full wave period. The formed vortices in each half cycle may travel a distance of $5d$ (Figure 4(c)).

It should be noted that only the dominant patterns, i.e. those seen in more than 40% of the cycles during the experiment duration of twenty periods, are indicated in Tables 1 and 2. Some other observations are worth noting here. Patterns may switch to other modes as already seen in time-dependent oscillatory flow [3,5]. The direction of shedding is not stable either. A little disturbance may change the wake mode and direction. This happens more frequently when KC is close to the upper limit of the range under consideration. At times, additional vortices form around the cylinder, in addition to the dominant wake pattern. Also, in some cases, a combination of vortex street and shooting mode was observed (e.g. in KC = 11.5 when $T = 1.14$ sec).

Another parameter that may change the flow pattern is wave steepness. For an identical KC number, the wakes tends to shed more in the direction of flow or switches to the lower KC pattern when the wave steepness decreases. For instance, the wake for KC = 11.5 and wave steepness of 0.5% tends to shed the vortex in the double-shooting mode, whereas, for the same KC, the wake sheds single-pair vortices when wave steepness is increased to 2.5%. The direction of shedding is not stable and little disturbance changes the wake direction. The Stokes and Reynolds numbers were not found to have significant effects on the flow pattern in the ranges examined here.

3.2. Dispersion around cylinder

We follow the technique described in Section 2.2 to examine dispersion of tracers virtually released into the flow at a distance of $2d$ from the cylinder. The numerical tests show that the dispersion is not affected by the time of release. Also, the results are not sensitive to the number of released particles. Figure 5 gives temporal variations of the longitudinal disper-

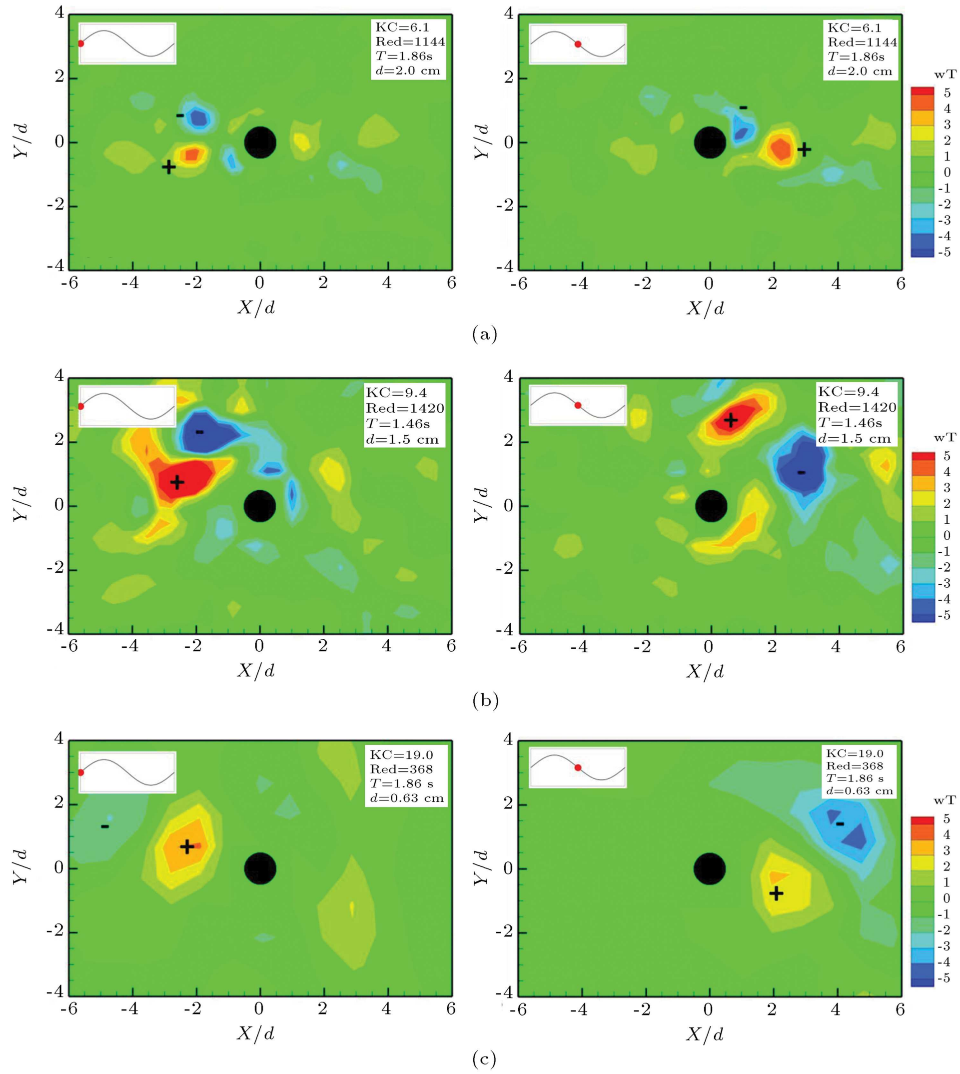

Figure 4. Non-dimensional vorticity fields around a single cylinder at the end of each half cycle in different flow patterns: (a) Double-shooting regime in $6 < \mathrm{KC} < 8$; (b) single-pair regime in $8 < \mathrm{KC} < 15$; and (c) double-pair regime in $15 < \mathrm{KC} < 24$.

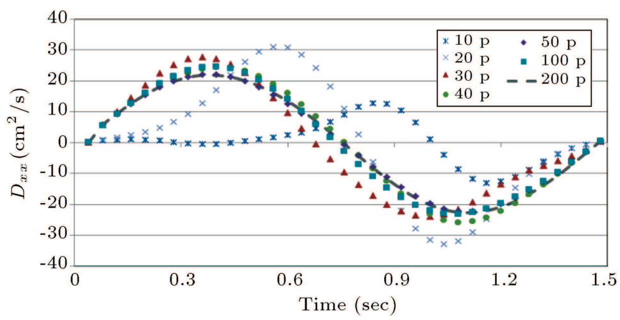

Figure 5. Sensitivity analysis of D_{xx} with respect to number of particles released.

sion coefficient, D_{xx}, from simulations, using different numbers of particles for a no-cylinder condition. The results almost coincide when the number of particles is bigger than 30. In the simulations to come, we release particles at an interval of 0.04 sec for a duration of $2T$, e.g. 93 particles for $T = 1.86$ sec. The first particle was released when the water depth started to increase from the mean level at the cylinder location. The start time was chosen such that the wake is in the dominant shedding pattern for a minimum of four wave periods.

Dispersion of mass around a cylinder in progressive wave motion changes with the vortex shedding pattern. Particle flow path changes when a particle reaches the cylinder neighborhood. Tracer particles released at a given point around the cylinder may take different trajectories. When the shedding intensity is high enough, tracers as far as $3d$ from the cylinder are absorbed into the vortex street. Figure 6 shows the particle trajectories realized for duration of $4T$ for the case of no-cylinder. Particle trajectories form a narrow line until the end of the fourth period. Particles positions at four instances in a period are shown in Figure 6. It shows that without molecular diffusion, the

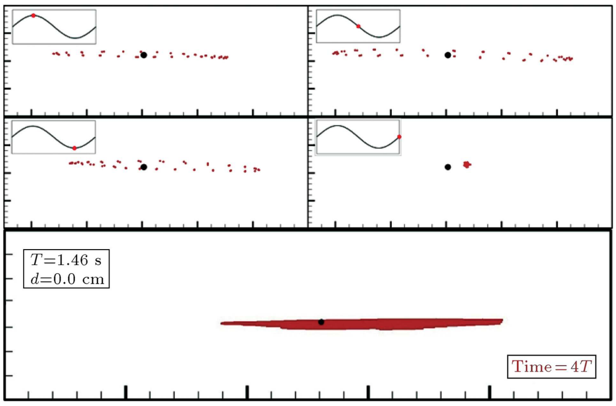

Figure 6. The particle positions at four instances during a period (above) and the related trajectories after four periods (below).

contribution of small transversal velocity fluctuations and shear effect in lateral dispersion is not significant in the flume in this case. The mass transport due to drift velocity can be observed in the particle trajectories in Figure 6.

Figure 7(a)-(c) show the particle trajectories around a cylinder for KC = 7.5, 9.4 and 22.7, respectively. These plots are representative of the three observed patterns, as discussed in Table 1. The plume generated from real release will be similar (but not identical) to the shape plotted in these figures [22]. When a cylinder is placed in the flow, vortex shedding affects the velocity field with both the mechanical diffusion and vortex shedding pattern contributing to dispersion. In a double-shooting regime, e.g. $6 < \mathrm{KC} < 8$, the vortices are weak and travel a maximum distance of $2d$. These vortices result in a weak local lateral flow, which disperses particles transversely (Figure 7(a)). In single-pair regime, i.e. $8 < \mathrm{KC} < 15$, the powerful vortex street pulls particles into the shedding path above the cylinder and the fluid particles move transversally while oscillating in a longitudinal direction (Figure 7(b)). Vortex shedding in the double-pair regime, i.e. $15 < \mathrm{KC} < 24$, is strong and has a direction changing between 0 and 45 degrees. This results in the patterns shown in Figure 7 (c).

Non-dimensional longitudinal and lateral covariances and dispersion coefficients for particles released from a point behind the cylinder are given in Figure 8(a)-(d). As expected, longitudinal dispersion is periodic in the no-cylinder case. Negative dispersion coefficient values indicate the tendency of the particles to shrink after expanding to a maximum amount at the end of a half cycle (e.g. see Figure 6). When a cylinder is placed in the flow, longitudinal dispersion is still periodic, but with an increasing amplitude for KC = 22.7 (double-pair regime) and KC = 11.7 (single-pair regime). This is due to the strong vortex shedding and collision of particles with the cylinder in these two

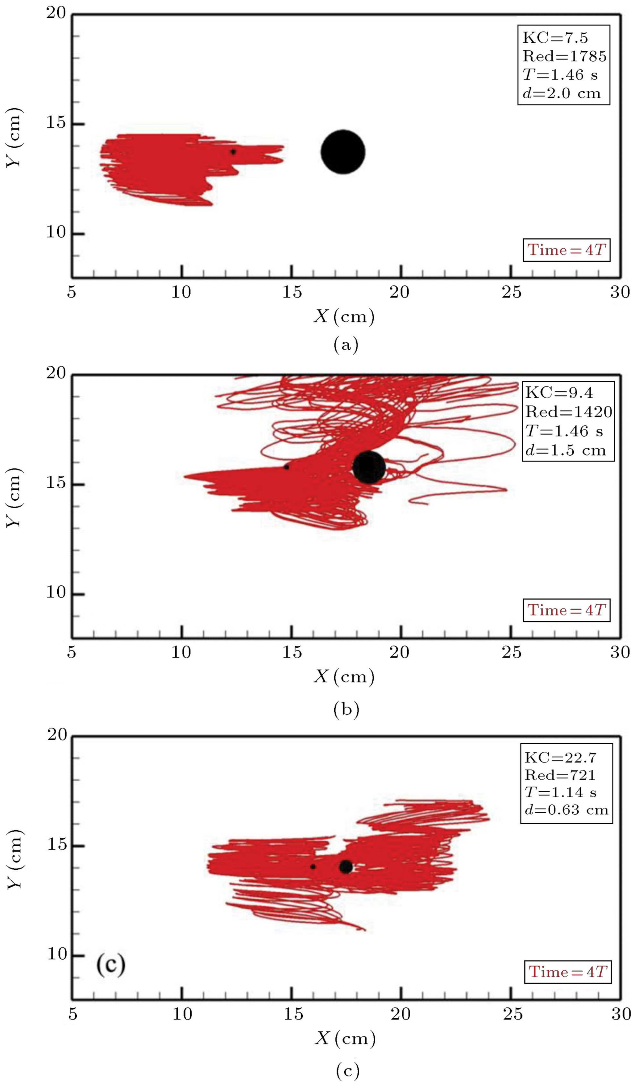

Figure 7. The particle trajectories around a single-cylinder for time of four periods after releasing.

cases. This is not the case, however, for KC = 6.1 (double-shooting regime). The longitudinal covariance and dispersion coefficient for this regime are even lower than those in the no-cylinder case. Fluid particles in this regime tend to expand more laterally and, so, dispersion along the wave direction is limited.

The lateral covariance and dispersion coefficient for a wave without a cylinder is very small. For all flow regimes around a circular cylinder, the lateral covariance increases with time. Maximum covariance and dispersion coefficients happen in a single-pair pattern with a transversal vortex street.

4. Concluding remarks

In this study, we investigated dispersion around an isolated circular cylinder in progressive wave motion, in the range $6 < \mathrm{KC} < 24$ and $20 < \beta < 310$. Flow fields and vortex shedding patterns were studied using si-

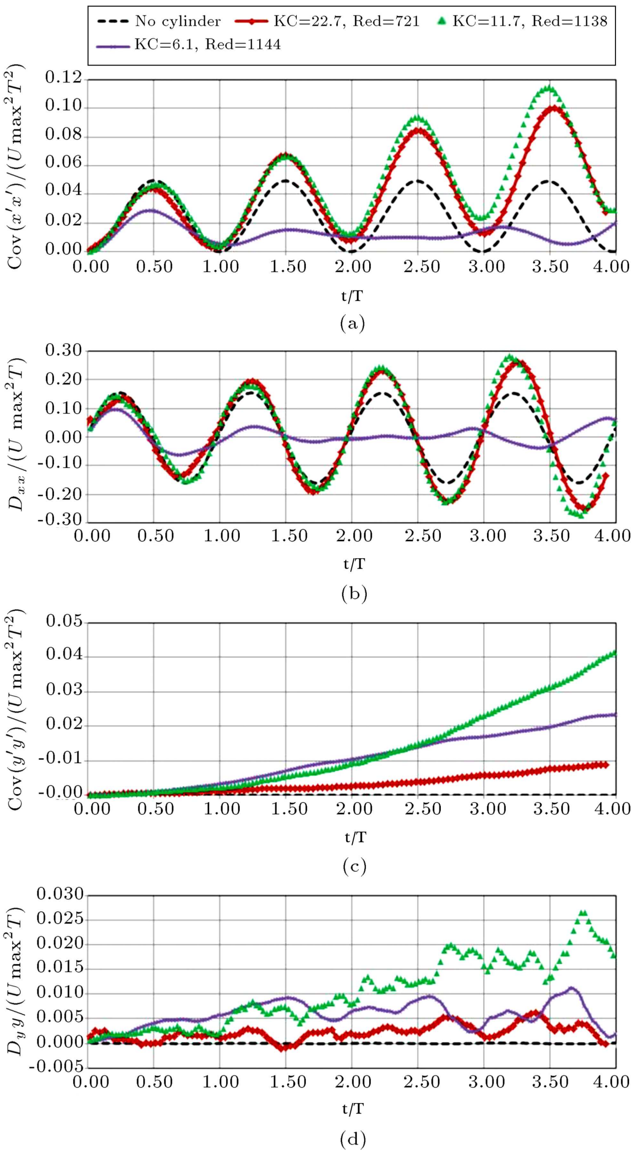

Figure 8. Non-dimensional (a) longitudinal covariances, (b) longitudinal dispersion coefficients, (c) lateral covariances and (d) lateral dispersion coefficients for particles released from a point behind the cylinder.

multaneous flow visualization and PIV measurements. Several repeatable patterns of vortex shedding around a single cylinder were detected. Double-shooting, single-pair, and double-pair shedding patterns were dominant in $6 < \mathrm{KC} < 8$, $8 < \mathrm{KC} < 15$ and $15 < \mathrm{KC} < 24$, respectively. We found that the vortex shedding patterns in progressive wave motion are similar to those observed in time-dependent oscillatory flow around a single cylinder with only little differences in the bounds of KC for given pattern. We also found that wave steepness may change the patterns. For a given KC, the wake tends to shed more in the direction of flow, or switches to the pattern corresponding to the lower KC range when wave steepness decreases. The direction of shedding is not stable and little disturbance changes the wake direction. The Stokes and Reynolds number have no significant effects on flow patterns at the ranges examined here. Experimental data shows that the Lagrangian dispersion method can well capture the dispersion patterns around a circular cylinder. Dispersion coefficients from this method encompass the main sources of dispersion, i.e. the effects of vortex shedding, mechanical, and shear dispersion. Furthermore, all four components of the planar dispersion tensor can be calculated at the same time by this method.

The subject still needs further work. As a subject for future research, the problem of dispersion around a group of cylinders has vast applications in dispersion in aquatic canopies, and can be studied using this technique. On the other hand, the technique needs to be refined to provide more reliable results. This requires more sophisticated equipment for flow visualization and more controlled experimental conditions. In our experiment, a weak transverse flow was occasionally observed, even when the cylinder was not in the flume. Although this looks to result from the use of a closed wave tank, one may want to eliminate any effect which is not present in the field.

References

1. An, H., Cheng, L. and Zhao, M. "Steady streaming around a circular cylinder in an oscillatory flow", *Ocean Engineering*, **36**, pp. 1089-1097 (2009).

2. Mendez, F.J. and Losada, I.J. "Hydrodynamics induced by wind waves in vegetation field", *Journal of Geophysical Research*, **104**(C8), pp. 18383-18396 (1999).

3. Williamson, C.H.K. "Sinusoidal flow relative to circular cylinders", *Journal of Fluid Mechanics*, **155**, pp. 141-174 (1985).

4. Bearman, P.W., Downie, M.J., Graham, J.M.R. and Obasaju, E.D. "Forces on cylinders in viscous oscillatory flow at low Keulegan-Carpenter numbers", *Journal of Fluid Mechanics*, **154**, pp. 337-356 (1985).

5. Obasaju, E.D., Bearman, P.W. and Graham, J.M.R. "A study of forces, circulation and vortex patterns around a circular cylinder in oscillating flow", *Journal of Fluid Mechanics*, **196**, pp. 467-494 (1988).

6. Tatsuno, M. and Bearman, P.W. "A visual study of the flow around an oscillating circular cylinder at low Keulegan-Carpenter numbers and low Stokes numbers", *Journal of Fluid Mechanics*, **211**, pp. 157-182 (1990).

7. Justesen, P. "A numerical study of oscillating flow around a circular cylinder", *Journal of Fluid Mechanics*, **222**, pp. 157-196 (1991).

8. Lin, X.W., Bearman, P.W. and Graham, J.M.R. "A numerical study of oscillatory flow about a circular cylinder for low values of beta parameter", *Journal of Fluids Structure*, **10**, pp. 501-526 (1996). doi: 10.1006/jfls.1996.0034

9. Saghafian, M., Stansby, P.K., Saidi, M.S. and Apsley, D.D. "Simulation of turbulent flows around a circular cylinder using nonlinear eddy-viscosity modelling: Steady and oscillatory ambient flows", *Journal of Fluids and Structures*, **17**, pp. 1213-1236 (2003).
10. An, H., Cheng, L. and Zhao, M. "Direct numerical simulation of oscillatory flow around a circular cylinder at low Keulegan-Carpenter number", *Journal of Fluid Mechanics*, **666**, pp. 77-103 (2011).
11. An, H., Cheng, L. and Zhao, M. "Steady streaming around a circular cylinder near a plane boundary due to oscillatory flow", *Journal of Hydraulic Engineering*, **137**(1), pp. 23-33 (2011).
12. Yasuda, H. "Longitudinal dispersion of matter due to the shear effect of steady and oscillatory currents", *Journal of Fluid Mechanics*, **148**, pp. 383-403 (1984).
13. Yasuda, H. "Longitudinal dispersion of matter due to the Stokes layer: Its time-dependence in the case of an instantaneous point-source", *Journal of the Oceanographical Society of Japan*, **44**, pp. 244-253 (1988).
14. Law, A.W.K. "Taylor dispersion of contaminants due to surface waves", *Journal of Hydraulic Research*, **38**(1), pp. 41-48 (2000).
15. Sumer, B.M., and Fredsøe, J., *Hydrodynamics Around Cylindrical Structures*, World Scientific, Singapore, RiverEdge, NJ. (1997).
16. Fischer, H., List, E., Koe, R., Imberger, J. and Brooks, N., *Mixing in Inland and Coastal Waters*, Academic Press, NY. (1979).
17. Nepf, H. "Drag, turbulence, and diffusion in flow through emergent vegetation", *Water Resources Research*, **35**(2), pp. 479-489 (1999).
18. Moroni, M. and Cushman, J.H. "Three-dimensional particle tracking velocimetry studies of the transition from pore dispersion to Fickian dispersion for homogeneous porous media", *Water Resource Research*, **37**(4), pp. 873-884 (2001).
19. Monin, A.S. and Yaglom, A.M., *Statistical Fluid Mechanics: Mechanics of Turbulence*, Cambridge, Mass.: MIT Press (1971).
20. Moroni, M., Cushman, J.H. and Cenedese, A. "A 3D-PTV two-projection study of pre-asymptotic dispersion in porous media which are heterogeneous on the bench scale", *International Journal of Engineering Science*, **41**, pp. 337-370 (2003).
21. Kundu, P., Cohen, I.M., *Fluid Mechanics*, Elsevier Academic Press, San Diego: Calif (2004).
22. Shavit, U. and Brandon, T. "Dispersion within emergent vegetation using PIV and concentration measurements", Presented at *4th International Symposium on Particle Image Velocimetry*, Gottingen, Germany, PIV 01 Paper P1129, pp.1-10 (2001).

Biographies

Mohammad Ali Tofighi received his MS degree in Civil Engineering (hydraulic structures, numerical modeling of water circulation and salinity dispersion in lakes) from Khajeh Nasireddin Toosi University of Technology (KNTU), Iran, in 2006. He is currently a PhD degree candidate of Civil Engineering (hydraulics) at Sharif University of Technology, Tehran, Iran. He is studying flow patterns and pollutant dispersion around circular cylinders and aquatic canopies under progressive wave motion.

Mirmosadegh Jamali received, respectively, MS degrees in Structural Engineering from Sharif University of Technology, Tehran, Iran, in 1990, and Applied Mathematics from the University of British Columbia, Canada, in 2000, from where he also obtained a PhD degree in Civil Engineering, in 1999. He is currently Associate Professor in the Department of Civil Engineering at Sharif University of Technology, Tehran, Iran. His primary research interests are environmental fluid mechanics and computational hydrodynamics.